Journal of Cellular Biochemistry 51:301–311 (1993)

Reduced Shear Stress: A Major Component in the Ability of Mammalian Tissues to Form Three-Dimensional Assemblies in Simulated Microgravity

T.J. Goodwin, T.L. Prewett, David A. Wolf, and G.F. Spaulding

KRUG Life Sciences (T.J.G., T.L.P.), NASA, Johnson Space Center (D.A.W., G.F.S.) Houston, Texas 77058

Abstract BHK-21 cells were cultured under various shear stress conditions in an Integrated Rotating-Wall Vessel (IRWV). Shear ranged from 0.5 dyn/cm^2 (simulated microgravity) to 0.92 dyn/cm^2. Under simulated microgravity conditions, BHK-21 cells complexed into three-dimensional cellular aggregates attaining 6×10^6 cells/ml as compared to growth under 0.92 dyn/cm^2 conditions. Glucose utilization in simulated microgravity was reduced significantly, and cellular damage at the microcarrier surface was kept to a minimum. Thus, the integrated rotating wall vessel provides a quiescent environment for the culture of mammalian cells. © 1993 Wiley-Liss, Inc.

Key words: integrated rotating-wall vessel, shear stress, simulated microgravity, three-dimensional tissues, microcarriers

The assembly of complex functional mammalian tissues is problematic due to the effects of shear stress, turbulence and inadequate oxygenation in conventional cell culture systems. This report describes the culture and three-dimensional assembly of baby hamster kidney (BHK-21) mammalian cells on microcarriers under controlled oxygenation, low shear stress, and turbulence in the NASA-designed integrated rotating-wall vessel (IRWV) (Schwarz and Wolf, 1991a). Anchorage-dependent cells are widely cultured on microcarriers (van Wezel, 1973). Studies show that for the purposes of improved surface-to-volume ratio and scale-up, the microcarrier suspension culture provides excellent potential for high density cell growth (Glacken et al., 1983). In addition, microcarriers serve well as structural supports for three-dimensional assembly, the composite of which is the basis for three-dimensional tissue growth (Goodwin et al., 1992).

Conventional culture systems for microcarrier cultures (i.e., bioreactors) use mechanical agitation to suspend microcarriers and thus induce impeller strikes as well as fluid shear and turbulence at the boundary layer between the wall and the fluid. Investigators have attempted to make a complete study of the most efficient bioreactor designs and agitation regimens (Croughan et al., 1987). They concluded that virtually all stirred-tank bioreactors operate in the turbulent regimen. It has been demonstrated that bead-to-bead bridging of cells is enhanced significantly at lower agitation rates in a stirred reactor (Cherry and Papoutsakis, 1988). Aggregates of as many as 12–15 microcarriers bridged with bovine embryonic kidney cells (BEK) have been reported.

Excessive agitation from either stirring or gas bubble sparging has been documented as a cause of cell damage in microcarrier cell cultures (Croughan and Wang, 1989a; Cherry and Hulle, 1992). To overcome the problems induced by these mechanisms, investigators developed alternative culture techniques such as porous microcarriers to entrap cells (Nilsson et al., 1986), increased viscosity of culture medium (Croughan et al., 1989b), bubble-free oxygenation (Thalman, 1989), and improved methods for quiescent inoculation (Clark et al., 1980; Feder and Tolbert, 1983). These steps decreased the damage attributed to turbulence and shear forces but failed to significantly rectify the problems. Reactor systems of substantially increased volume exhibit less agitation-related cell damage.

Received September 25, 1992; accepted October 15, 1992.

Address reprint requests to Dr. T. J. Goodwin, KRUG Life Sciences, 1290 Hercules Drive, Suite 120, Houston, TX 77058.

This is presumably due to the decreased frequency of cell/microcarrier contact with the agitation devices in the systems.

Research scale investigations do not afford the luxury of experimenting with large scale production systems. Therefore, if a large-volume system is indeed more quiescent, an improved bioreactor system should emulate the fluid dynamics present in the upper regions of large-scale reactors in which cells and microcarriers reside with minimal agitation.

Microcarriers and cells in large-volume reactors are semibuoyant rendering them practically weightless, a condition that we hypothesize may be analogous to the environment of microgravity. It is stated that "Unless a cell culture is growing in an environment free of gravitational forces, moderate levels of agitation are required to suspend microcarriers that are not neutrally buoyant" (Croughan et al., 1989b). The ability to grow cells in a rudimentary horizontally rotated chamber has been previously demonstrated (Briegleb, 1983). This configuration was intended to simulate in the laboratory the effects of weightlessness or microgravity on cells. It was shown that human embryonic kidney (HEK) cells attach to microcarriers in microgravity (Space Shuttle experiment) and that attachment and spreading may be enhanced in a weightless environment (Tschopp et al., 1984). Review articles of cell biology performed in space flight experiments delineate the growth of many cell types in an environment devoid of gravitational influence (Gmuender and Cogoli, 1988; Goodwin et al., 1988). The problem, then, is to suspend microcarriers and cells without inducing turbulence or shear while providing adequate oxygenation and nutritional replenishment. One environment that possesses these attributes is the microgravity of space flight. Another is the system referenced here which randomizes the forces of gravity by classical methods, thus simulating some aspects of microgravity.

The term rotating-wall vessel (RWV) comprises a family of vessels, batch fed (Fig. 1) and perfused (Fig. 2), which embody the same fluid dynamic operating principles. These principles are (1) solid body rotation about a horizontal axis which is characterized by (a) co-location of particles of different sedimentation rates, (b) extremely low fluid shear stress and turbulence, and (c) three-dimensional spacial freedom; and (2) oxygenation by active or passive diffusion to the exclusion of all but dissolved gasses from the reactor chamber, yielding a vessel devoid of gas bubbles and gas/fluid interface (zero headspace) (Wolf and Schwarz, 1991; Schwarz et al., 1992).

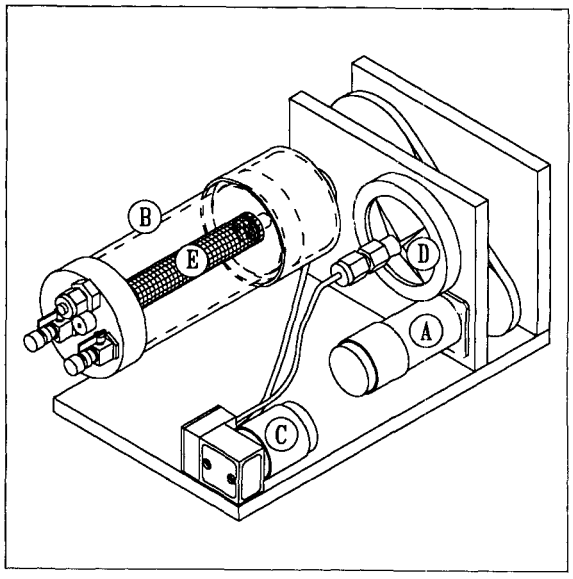

Fig. 1. Schematic of the RWV A 24-VDC motor (**A**) drives a belt that rotates the culture vessel (**B**) around its horizontal axis An air pump (**C**) draws incubator air through a 0 22-μm filter (**D**) and discharges it through a rotating coupling on the shaft that carries the vessel The air pump moves about 1 L/min of air The oxygenator membrane (**E**) is wrapped around the center post The vessel end caps and wall are made of lexan

The horizontally rotating culture vessel simulates some aspects of microgravity (Dedolph and

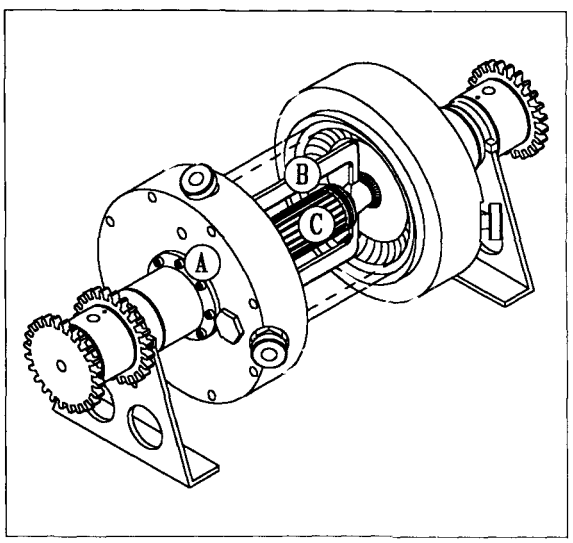

Fig. 2. Schematic of the IRWV with three axes of rotation exhibited The wall of the culture vessel (**A**), the vane (**B**), and the spin filter (**C**) are shown The spin filter is covered with 50 micron polyester cloth to prevent loss of microcarriers and cellular material into the perfusion loop

Dipert, 1971; Schwarz et al., 1992; Prewett et al., 1993) reducing to a minimum the shear and turbulence associated with impeller-driven, stirred bioreactors. Microcarriers and cells remain uniformly suspended in the fluid. Shear forces and mass transfer in solid body rotation are attributed to the minute movements of the microcarriers in the medium and their incidental contact with the wall and one another.

Conventional methods of oxygenation disturb the medium and damage the cells (Cherry and Kwon, 1990; Cherry and Hulle, 1992). Previous designers have suspended particles in a quiescent environment by horizontal rotation (Vaseen, 1980); however, none has been able to provide a means of oxygenation that does not perturb this tranquil environment. Many stirred reactors depend on gas control and diffusion at the gas/medium interface (headspace oxygenation). Many others use sparging or air lift techniques where gas is introduced as minute bubbles and thus lift the cells and microcarrier up through the medium.

The use of silicone rubber tubing to oxygenate a 14-liter bioreactor has been previously explored (Fleischaker and Sinsky, 1981). In this method silicone rubber tubing was placed in direct contact with the medium. A gas mixture was circulated through the tubing diffusing into the medium at the coefficient of the particular gas (passive diffusion). They found that oxygen transport varied with the rate of agitation and concluded that the problem of oxygenation in large-scale cell culture could be adequately dealt with by membrane oxygenation. Gas diffusion through a silicone membrane can be improved by decreasing the membrane thickness. An example of this current technology is extracorporeal oxygenators used in heart–lung machines. The batch-fed RWVs use this method of oxygenation (Schwarz et al., 1991b) (Fig. 1A), employing a centrally located silicone membrane for transfer of dissolved gasses (Schwarz et al., 1992). Incubator air is circulated through the center shaft of the vessel via an external air pump, thus eliminating induction of air bubbles into the culture medium (Fig. 1E). The IRWV uses a membrane in the vessel for the retention of cellular material and passage of return medium to the perfusion loop (Fig. 2C). This loop passes through a sensor block that analyzes dissolved oxygen (dO_2), dissolved carbon dioxide (dCO_2), pH, glucose and temperature, then to an in-line hollow fiber oxygenator that revitalizes the medium with the proper $dO_2/dCO_2/dN_2$ gas balance. Additionally, the IRWV is constructed to permit three independent horizontal axes of rotation, i.e., the wall, the vane, and the spin filter (Fig. 2A–C). Three-axis rotation allows the addition of minute levels of shear stress to be added to desired cell cultures or, in this study, to determine the effects of increasing shear stress and turbulence on the growth and three-dimensional assembly of mammalian cells. The results presented herein demonstrate that BHK-21 cells propagated for 7 days in an IRWV exhibited deleterious effects when subjected to fluid shear stresses of 0.92 dyn/cm^2.

MATERIALS AND METHODS

Cell Line

Baby hamster kidney (BHK-21) cells were obtained from the American Type Culture Collection (ATCC) (Rockville, MD). Cells were cultured in an enriched medium identified as microcarrier medium (MM) developed at NASA/Johnson Space Center (Table I). BHK cells were grown in Corning T-150 flasks up to passage 56 prior to inoculation into vessels. All cells were previously screened for *Mycoplasma* contamination and were certified negative.

Description of Hardware and Culture Conditions

The IRWV used in these experiments was designed as outlined in U.S. Patent 4,988,623 (Schwarz and Wolf, 1991a). The unit consists of a 500-ml horizontally rotated cylinder with three

TABLE I. Microcarrier Medium Complete

Medium	Manufacturer/no.	Quantity
Medium 199	(Gibco 400-1100EB)	1.0 pkg/3 L
MEM-Alpha	(Gibco 410-1900EB)	1.0 pkg/3 L
D-MEM	(Gibco 430-2100EB)	1.0 pkg/3 L
$NaHCO_3$	(Sigma S5761)	6.048 g/3 L
Bactopeptone	(Difco 0118-01-8)	1.2 g/3 L
Folic acid	(Sigma F-8758)	0.02 g/3 L
i-Inositol	(Sigma I-7508)	0.072 g/3 L
Nicotinic acid	(Sigma N-0761)	2.0 ml/3 L of 50-mg/dl stock
HEPES	(Research Organics 6003H-2)	14.298 g/3 L
Pen-Strep	(Gibco 600-5145 AE)	10.0 ml/L
Fungizone	(Gibco 600-5295 AE)	10.0 ml/L
NaOH	(pH adjusted with 1 N NaOH)	20.0 ml/3 L of 1N stock
Fetal calf serum	(Hyclone A-1111-L)	100.0 ml/L

independent axes of rotation; the wall, the vane and the spin filter (Fig. 2). The vessel employs an external perfusion loop that permits the on-line monitoring and addition of O_2, CO_2, glucose and NaOH for pH control (Fig. 3). The vessel was completely filled with MM (Table I), inoculated through a syringe port with Cytodex-3 microcarriers (average size is 175 μm), then inoculated with BHK-21 cells at a concentration of 10 cells/microcarrier. Microcarrier concentration was 5 mg/ml (4,000 beads/mg) yielding approximately 2×10^5 cells/ml. Vessel rotation was initiated and maintained at 20 rpm without perfusion for the first 24 hours to allow appropriate cell attachment to the microcarriers. Thereafter, the vessel was perfused with a 67% medium change each 24-hr period to replenish nutrients.

Vessel fluid dynamics in solid body rotation were described previously for this vessel (Wolf and Schwarz, 1991; Tsao et al., 1992) and for non-perfused RWV's (Schwarz et al., 1992; Prewett et al., 1993). To demonstrate the lowest discernible level of damaging fluid shear on three-dimensional cell to microcarrier assembly, experiments were conducted at calculated shear stresses ranging from 0.51 dyn/cm^2 (solid body rotation) to 0.92 dyn/cm^2 (Tsao et al., 1992; Wolf and Schwarz, 1992). This was achieved in the IRWV by placement of the vane 6.35 mm from the vessel wall and in the case of sheared experiments using a different rate of rotation between the vessel wall and the vane.

Growth Curves

Initial samples were harvested at approximately 48 hr and thereafter each 24-hr period to assess the progress of the cultures and determine the total cell count and viability. Analysis for total numbers of cells was performed by the previously described method (Sanford et al., 1951; Schwarz, et al., 1992; Goodwin et al., 1993).

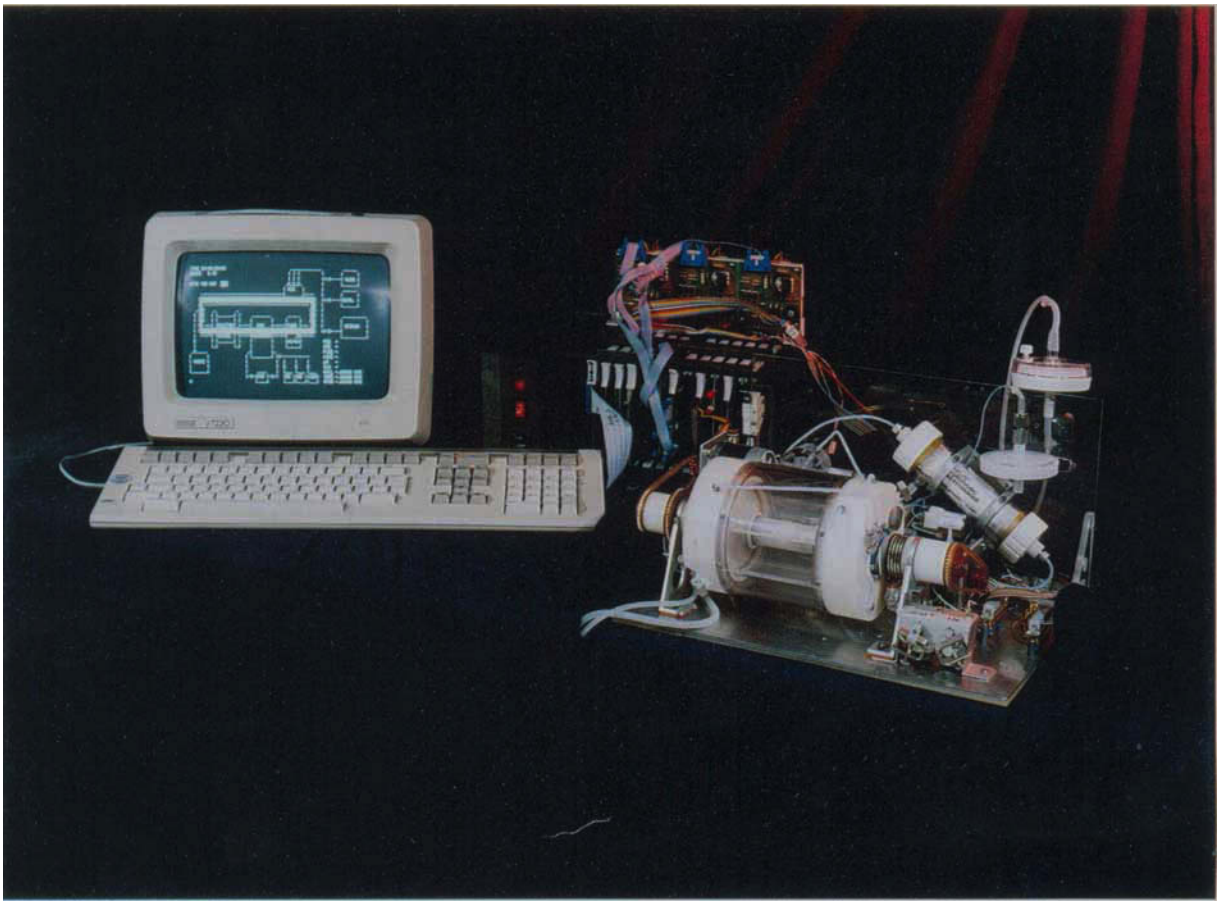

Fig. 3. Photograph of computer-controlled IRWV system as configured for these studies Left to right are the CRT and keyboard, the computer module and drives (external to incubator), and the vessel deck containing the IRWV, sensor block, and perfusion loop (internal to incubator)

Briefly, three 1-ml cell/microcarrier samples were removed from the vessel, washed twice with calcium and magnesium free (CMF)–PBS, transferred to a 1-ml solution of 0.1% crystal violet/0.1 M citric acid and vortexed, then incubated at 37°C for 1 hr. Released nuclei were enumerated by hemacytometer and microcarriers were counted in a model M Coulter Counter with a 560-nm aperture. Numbers of nuclei were first converted to cells/microcarrier then to cells/ml. Cellular viability was determined by trypan dye exclusion.

Three-Dimensional Aggregation

Three-dimensional aggregation of BHK-21 cells was determined beginning at 48 hr and continued each 24-hr period thereafter. Three 1-ml samples of cell-microcarrier aggregates were taken, then transferred into 35 mm petri dishes with 2 mm grids (Lab-Tek Division, Miles Laboratories, Cat. No. 5217) and were evenly dispersed for counting. The number and size of the aggregates were determined over ten 2-mm-square grids. The percentage of aggregates was calculated, averaged over three counts, and grouped in the following categories: 2–5 microcarriers. 6–15 microcarriers, and > 16 microcarriers per aggregate.

Scanning Electron Microscopy

Cell/bead samples were removed from the IRWV as stated above and fixed in a solution containing 3% glutaraldehyde and 2% paraformaldehyde in 0.1 M cacodylic buffer, pH 7.4. Samples were prepared for scanning electron microscopy as previously described (Goodwin et al., 1992, 1993; Schwarz et al., 1992; Prewett et al., 1993). Briefly, samples were rinsed with cacodylate buffer, fixed with 1% OsO_4 in cacodylate buffer, rinsed and fixed with 1% TCH. Samples were then rinsed again, fixed with 1% OsO_4, and dehydrated with increasing concentrations of ethanol. Samples were critical point dried and scanned on a JOEL model T330 electron microscope at 5 kV.

Metabolic Data

Metabolic data were collected during the experiments to assess the effects of shear stress on the assembly of cell/microcarrier aggregates. Media samples were harvested as stated above for analysis of glucose, dO_2, dCO_2, pH, and enzymatic assays. Glucose, dO_2, dCO_2, and pH were analyzed off line by a Corning 168 Blood Gas Analyzer and Beckman Glucose Analyzer 2, respectively. Analysis of specific enzymatic activity including Alanine Transaminase (SGPT), Asparagine Transaminase (SGOT), Lactate Dehydrogenase (LDH), and Alkaline Phosphatase were accomplished with a Beckman Synchron CX5.

RESULTS

Growth Curves

BHK-21 cells were cultured for 7 days in triplicate experiments; the results of these experiments are detailed in Figure 4. The growth curves demonstrate a significant impairment of BHK-21 cells to grow and develop normally under shear conditions of 0.92 dyn/cm^2. Conversely, solid body rotation or near solid body rotation at 0.51 dyn/cm^2 in the IRWV produced robust cultures, which grew to a maximum cell number of 6×6^{10} cells/ml. During the course of all experiments, dO_2, dCO_2, and pH were monitored closely. CO_2 was kept to a maximum of 40 mm Hg, oxygen was kept above 65 mm Hg, and pH was never allowed to drop below 6.9. Cell viability was determined by standard trypan blue dye exclusion assay (Goodwin et al., 1992).

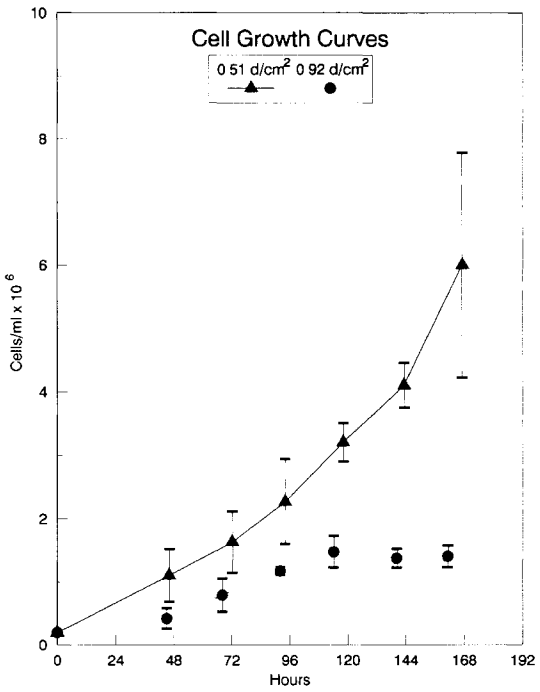

Fig. 4. The average of triplicate experiments conducted at 0.51 and 0.92 dyn/cm^2. Cells in the 0.51 dyn/cm^2 experiments attained an average of 6×10^6 cells/ml, while experiments conducted under 0.92 dyn/cm^2 resulted in reduced proliferation.

Three-Dimensional Aggregation

Figure 5 demonstrates the difference in cell growth and three-dimensional assembly under experimental conditions of 0.51 dyn/cm^2 versus 0.92 dyn/cm^2 fluid shear stress. The distribution of aggregate assembly was not statistically different in the early phase of the experiments where microcarrier bead packs ranged from two to five microcarriers in number (Fig. 5A). However, as the experiments progressed, a significant difference in the ability of microcarriers and cells to complex into larger three-dimensional aggregates was observed. Figure 5B demonstrates a significant divergence in the range of 6–15 microcarrier aggregates between condition 0.51 and 0.92 dyn/cm^2. Less than 20% of the total number of aggregates at 0.92 dyn/cm^2 at 94 hr were in the range of 6–15 microcarrier aggregates. Conversely, in the shear condition of 0.51 dyn/cm^2, greater than 45% of the aggregates had attained a size of 6–15 microcarriers. This trend continued throughout the duration of the cultures at 0.51 dyn/cm^2. Although the aggregate sizes continued to increase marginally under 0.92 dyn/cm^2 shear, severe impairment in the cell-microcarrier assembly process was evident. Figure 5C further demonstrates the inability of BHK-21 cells to aggregate and complex into three-dimensional tissues at a shear level of 0.92 dyn/cm^2. Fewer than 10% of the aggregates of greater than 16 microcarriers in size were evident in the high shear condition. However, starting at 94 hr and continuing through the termination of the cultures, aggregates of greater than 16 were present in the 0.51-dyn/cm^2 conditions.

Scanning Electron Microscopy

The degree and intensity of cellular damage at 0.92 dyn/cm^2 was particularly evident when compared photographically to conditions at 0.51 dyn/cm^2. Figures 6 and 7 are two panels of scanning electron micrographs that compare shear conditions. Figure 6 compares photographs at a magnification of ×350. Figure 6A,C,E demonstrates the normal growth of BHK-21 cells under 0.51 dyn/cm^2 shear at 46, 94, and 167 hr, respectively. Damage to the three-dimensional aggregation of microcarrier packs is apparent in Figures 6B,D,F and 7B,D,F (magnification ×750). Clearly, 0.92 dyn/cm^2 shear inhibits the formation and continued progress of cells growing on the surface of three-dimensional bead packs.

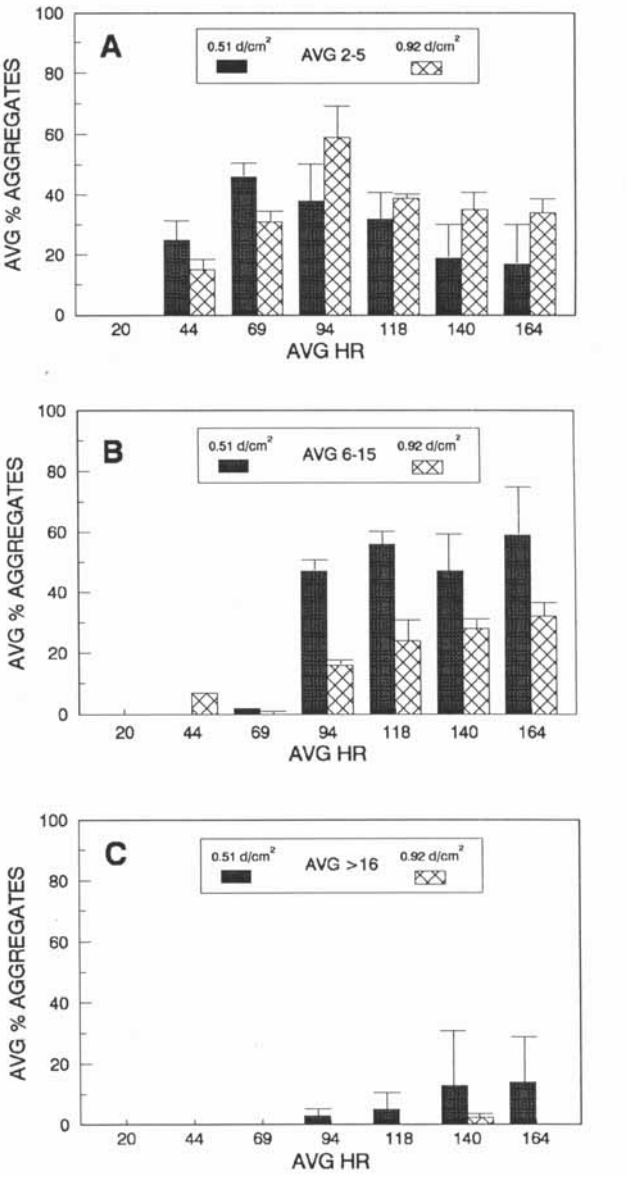

Fig. 5. Histograms of the average percent aggregate data for 0.51 dyn/cm^2 and 0.92 dyn/cm^2 A–C Note the reduced aggregation in the condition of 0.92 dyn/cm^2 per sample Totals do not equal 100% due to the percentage of single microcarriers not graphed

Metabolic Data

Glucose utilization was calculated for each set of triplicate experiments at 0.51 and 0.92 dyn/cm^2. After an initial spike under both experimental conditions, glucose utilization in the 0.51-dyn/cm^2 experiments decreased from approximately 11 mg/dl/cell/hr × 10^{-9} to <4 mg/dl/cell/hr × 10^{-9} at the end of the experiments (Fig. 8). Alternatively, the consumption of glucose in the 0.92 dynes/cm^2 condition increased significantly, beginning at 96 hr and continuing

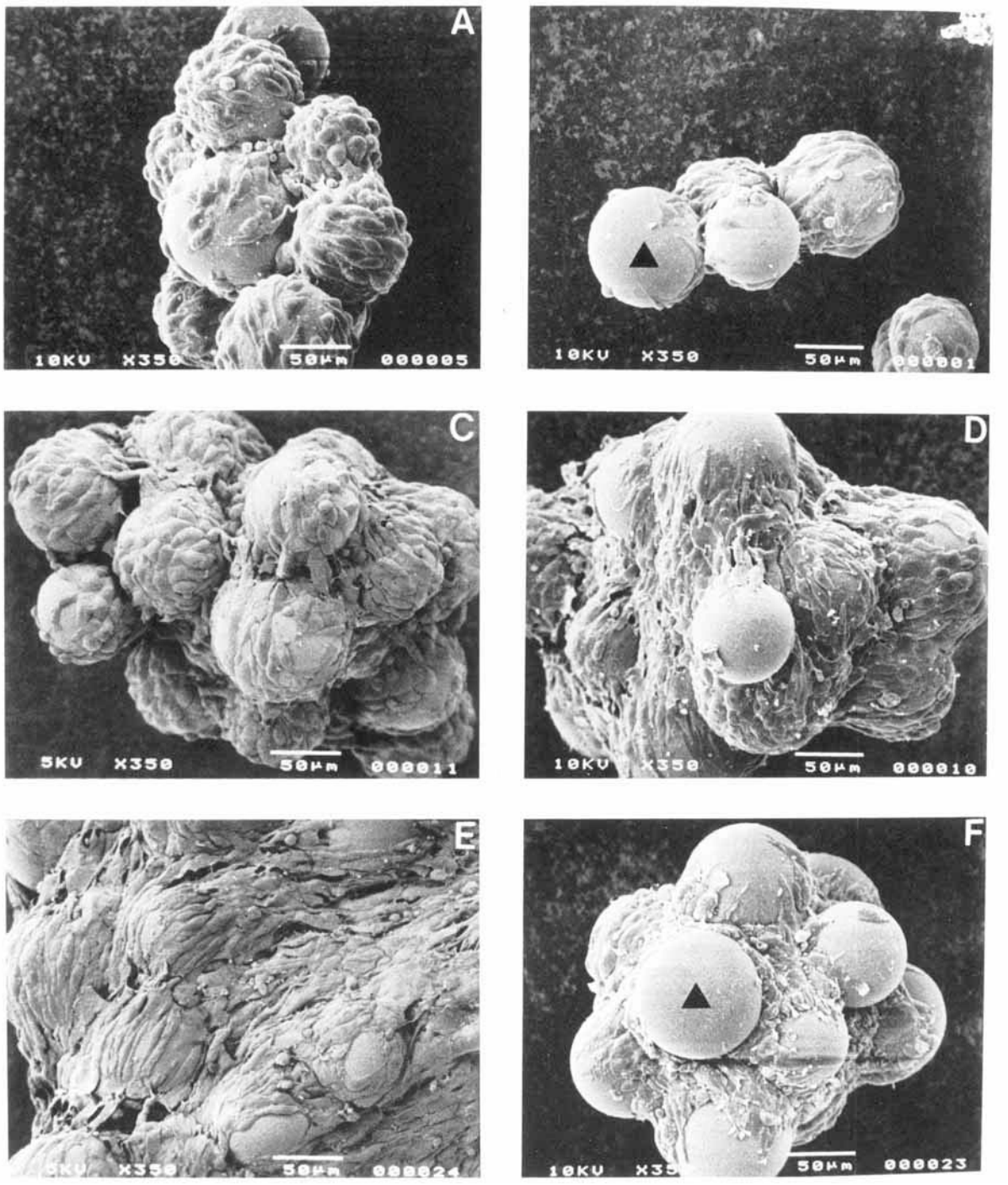

Fig. 6. Scanning electron micrographs (×350) of condition 0 51 dyn/cm^2 **(A,C,E)** and condition 0 92 dyn/cm^2 **(B,D,F)** At 46 (A,B), 94 (C,D) and 167 (E,F) hr Microcarriers are indicated with a triangle (B,F) Note the confluent microcarriers in C as compared to D Note the condition of the cells on the bead and the size of the aggregate in E as compared with 6F, which exhibits microcarriers and cells generally in poor condition

through 168 hr. At this point, the level of glucose consumption on a per-cell basis was near 15 mg/dl/cell/hr × 10^{-9}. A panel of enzymatic levels (alkaline phosphatase, SGOT, SGPT, and LDH) was analyzed to determine the metabolic state of the cells during each experiment. Figure 9A demonstrates the level of alkaline phosphatase at 0.51 and 0.92 dyn/cm^2. These data indicate that neither of the conditions elicited a significant increase in the amount of released

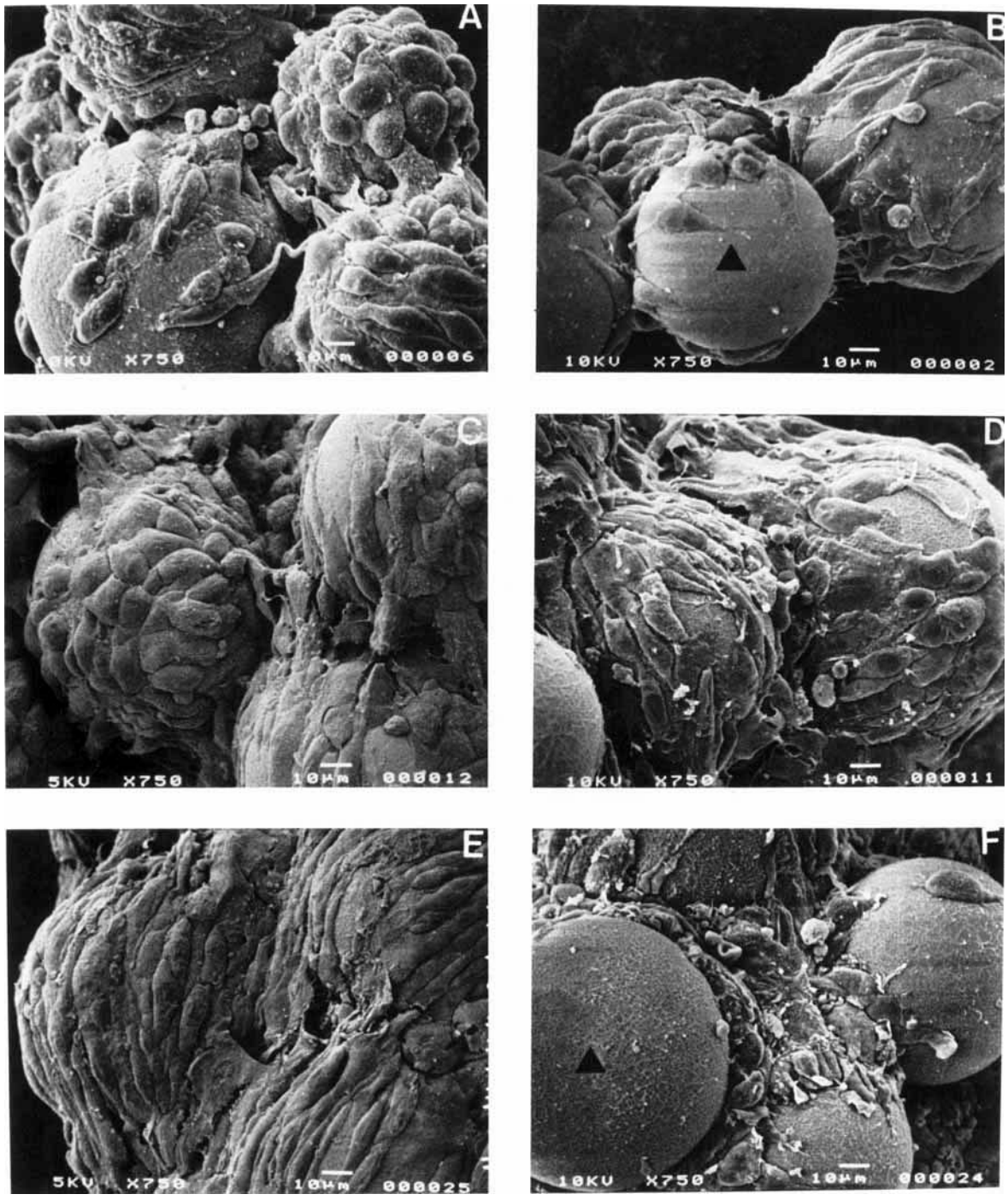

Fig. 7. Scanning electron micrograph (×750) of conditions outlined in Figure 6. Again, note the bare microcarriers (triangle) in 7F. Cells are shown growing in the crevices of the bead pack of F, while E displays a healthy culture that has attained confluence on the microcarriers.

alkaline phosphatase. Figure 9B demonstrates the amount of released SGPT in the 0.51- and 0.92-dyns/cm^2 experiments. The 0.92 dyn/cm^2 did result in significantly elevated levels of SGPT beginning at 96 hr and continuing throughout the end of the experiments. Figure 9C demonstrates the release of SGOT in the two experimental conditions. Levels of SGOT declined initially in the 0.51 dyn/cm^2 condition and continued to decline throughout the duration of the experiments. However, at 96 hr, the period at which large numbers of microcarriers began

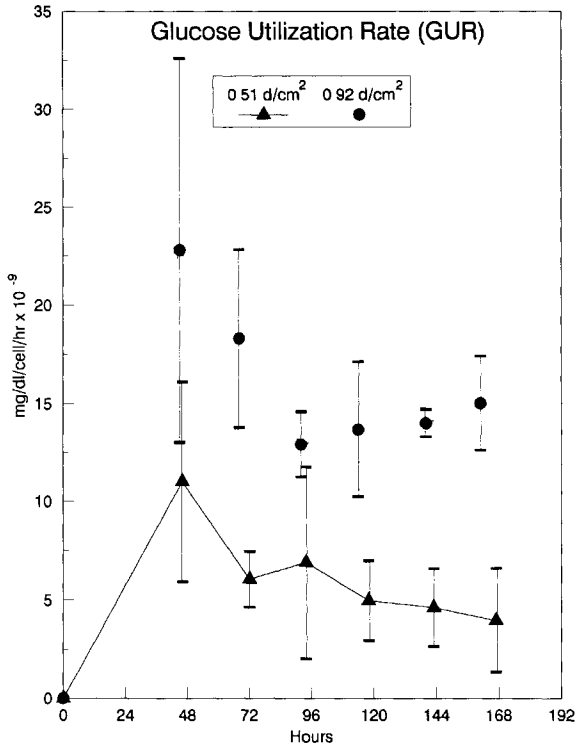

Fig. 8. Graph of glucose utilization rates of condition 0.51 dyn/cm^2 and 0.92 dyn/cm^2. Note the glucose consumption per cell decreases in condition 0.51 dyn/cm^2 and increases in condition 0.92 dyn/cm^2.

to complex into larger three-dimensional aggregates, a significant release of SGOT is evident in the cultures, and this release continues to increase throughout the remainder of the experiment. Figure 9D shows a significant difference in the amount of released LDH between the conditions of 0.51 dyn/cm^2 and 0.92 dyn/cm^2 shear stress. A significant divergence of the two curves occurs at 96 hr into the cultures. LDH increased and continued to increase throughout the remainder of the experiment in the 0.92 dyn/cm^2 conditions. Finally, 0.51 dyn/cm^2 effected no change and actually resulted in a small decrease in the amount of released LDH.

DISCUSSION

Several interesting phenomena are revealed upon review of these data. First, BHK-21 cells respond negatively when exposed to relatively low levels of fluid shear stress. The literature cites levels of shear stress in the range of 3–10 dyn/cm^2 (Cherry and Papoutsakis, 1986) as being sufficient to inflict damage to cells. In our studies, although large-scale cell lysis did not occur, the capability of the cells to reach their maximum cell number was significantly impacted and, clearly, three-dimensional assembly on microcarriers was curtailed. Figure 5B,C shows a striking difference between simulated microgravity cultures at 0.51 dyn/cm^2 and the shear stress of 0.92 dyn/cm^2. Three-dimensional assemblies are suppressed at the higher shear stress and even those aggregates that do form exhibit signs of severe damage (Figs. 6, 7B,D,F). Inspection of Figures 6 and 7 makes apparent the effect of shear at the microcarrier surface. Cells in the 0.92 dyn/cm^2 condition are seen growing in between the microcarriers but fail to inhabit the outer areas.

Damage to cells at low levels of shear is concomitant with the release of biomolecules from within the cells which arrest both the proliferative and structural functions of the cells. Figure 8 expresses the amount of glucose consumed on a per cell basis. Under conditions of 0.51 dyn/cm^2 or simulated microgravity, BHK-21 cells used approximately 60–70% less glucose and attained cell numbers of more than 6×10^6 cells/ml. However, under 0.92 dyn/cm^2 shear stress the cells failed to proliferate and aggregate well, indicating sensitivity to these conditions and inefficient use of the available energy sources. Further evidence of damage and arrested ability to function in relatively low shear is confirmed by the data presented in Figure 9A–D. The release of intracellular enzymes (LDH, SGOT, SGPT, and alkaline phosphatase) under conditions of shear indicates at least minimal damage to the cellular membranes. This low-level damage may require the cell to channel energy into repair efforts rather than into cellular proliferation and structural assembly. The data indicate an inability of the cultures to overcome continued shear stress at 0.92 dyn/cm^2. As the cultures begin to complex, shear may artificially restrict the size and complexity of the microcarrier-cell aggregates.

The composition of the factors outlined above may indeed explain the decreased use of glucose at 0.51 dyn/cm^2 and the increased use of glucose at 0.92 dyn/cm^2 shear stress. The data confirm the benefit of reduced shear or simulated microgravity as a constructive tool in the assembly of three-dimensional tissues.

Coincidentally, subsequent studies that are under way in our laboratories indicate variances in the consumption and production of certain basic amino acids known to be important in

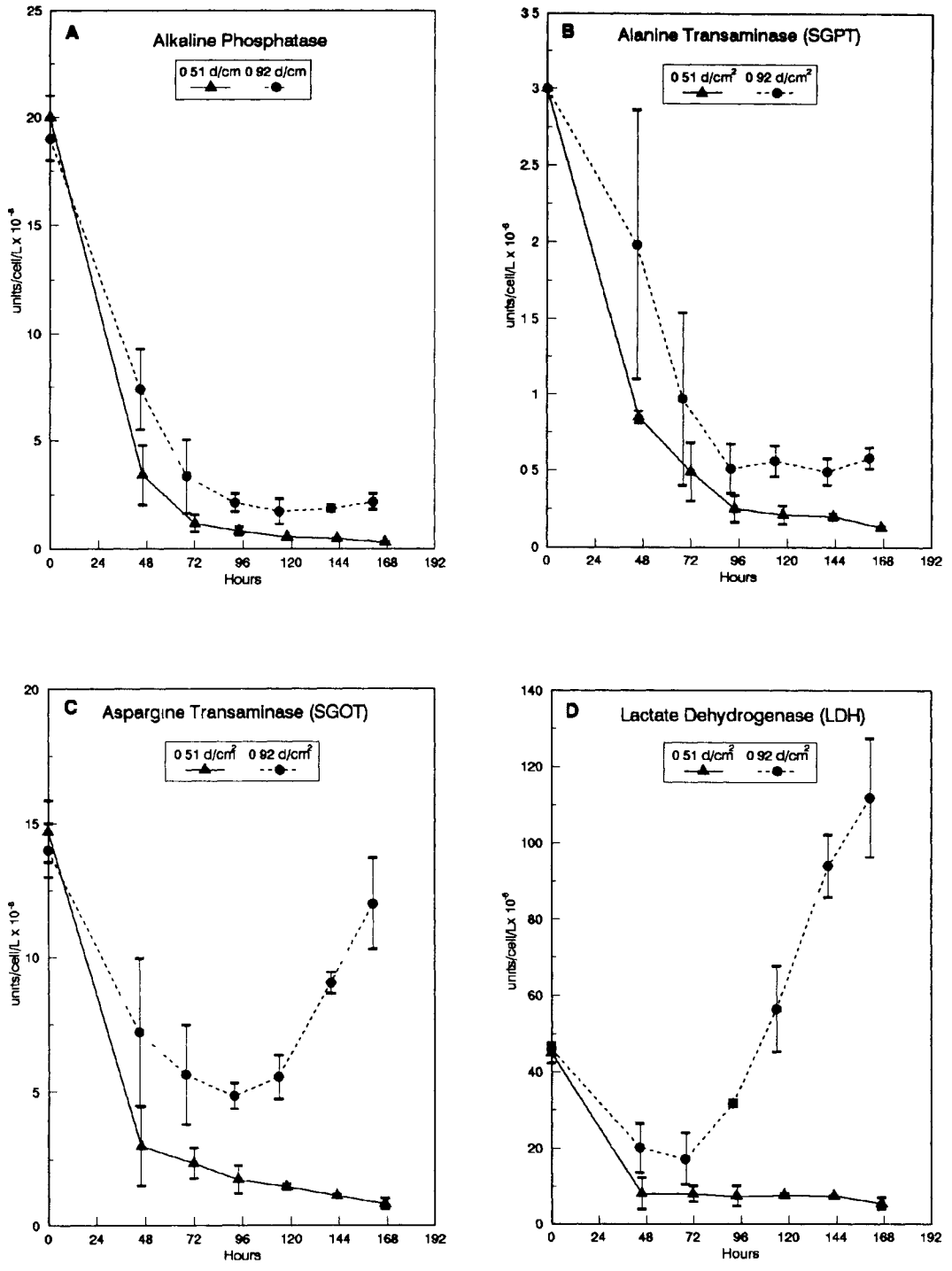

Fig. 9. Graphs of enzyme analysis SGPT (B), SGOT (C), Alkaline Phosphatase (A), and LDH (D), for condition 0 51 dyn/cm^2 and condition 0 92 dyn/cm^2 Note that SGPT increases slightly for 0 92 dyn/cm^2, while it decreases from 0 51 dyn/cm^2 SGOT and LDH levels increase dramatically under conditions of 0 92 dyn/cm^2 shear, while they decrease under 0 51 dyn/cm^2 shear stress

secondary metabolism (Rodwell, 1981). The most notable of these are the large increases in glycine, alanine and ornithine in the 0.51-dyn/cm^2 shear condition. These amino acids all share common lineage in the gluconeogenic pathway found almost exclusively in the mammalian liver and kidney (Lehninger, 1975). Efficient use of glucose and other available energy sources in functional tissues would reduce the overall glucose consumption in these cultures.

In summary, conditions of extremely low shear stress (0.51 dyn/cm^2) simulate some aspects of microgravity and may be analogous to characteristics of actual microgravity, fostering a quiescent environment in which cells may devote energy utilization to structural and functional aspects of three-dimensional tissue growth.

ACKNOWLEDGMENTS

The authors thank Ms. Kay Henry for her expert technical assistance and Ms. Carolyn Rogan for her efforts in the preparation of this manuscript. This work has been supported by NASA Microgravity Science and Applications division Contract NAS9-18492.

REFERENCES

Briegleb W (1983) The clinostat—a tool for analyzing the influence of acceleration on solid-liquid systems Proceedings of Workshop on Space Biology, Cologne, Germany (ESA SP-206) 1983 97–101

Cherry RS, Papoutsakis ET (1986) Hydrodynamic effects on cells in agitated tissue culture reactors Bioproc Eng 1 29–41

Cherry RS, Papoutsakis ET (1988) Physical mechanisms of cell damage in microcarrier cell culture bioreactors Biotechnol Bioeng 32 1001–1014

Cherry RS, Kwon KY (1990) Transient shear stresses on a suspension cell in turbulence Biotechnol Bioengineer 36 563–571

Cherry RS, Hulle CT (1992) Cell death in the thin films of bursting bubbles Biotechnol Prog 8 11–18

Clark J, Hirtenstein M, Gebb C (1980) Critical parameters in the microcarrier culture of animal cells Dev Biol Standard 46 117–124

Croughan MS, Hammel JF, Wang DIC (1987) Hydrodynamic effects on animal cells grown in microcarrier cultures Biotechnol Bioeng 29 130–141

Croughan MS, Wang DIC (1989a) Growth and death in overagitated microcarrier cell cultures Biotechnol Bioeng 33 731–744

Croughan MS, Sayre SS, Wang DIC (1989b) Viscous reduction of turbulent damage in animal cell culture Biotechnol Bioeng 33 862–872

Dedolph RR, Dipert MH (1971) The physical basis of gravity nullification by clinostatic rotation Plant Physiol 47 756–764

Feder J, Tolbert WR (1983) The large-scale cultivation of mammalian cells Sci Am 248 36–43

Fleischaker RJ, Sinsky AJ (1981) Oxygen demand and supply in cell culture Eur J Appl Microbiol Biotechnol 12 193–197

Glacken MW, Fleishaker RJ, Sinsky AJ (1983) Mammalian cell culture engineering principles and scale-up Trends Biotechnol 1 102–108

Gmuender FK, Cogoli A (1988) Cultivation of single cells in space Appl Microgravity Technol 1 115–222

Goodwin TJ, Jessup JM, Sams C, et al (1988) In vitro three-dimensional tissue modeling J S C Technology Annual Report, NASA Technical Memorandum 100473

Goodwin TJ, Jessup JM, Wolf DA (1992) Morphologic differentiation of colon carcinoma cell lines HT-29 and HT-29KM in rotating-wall vessels In Vitro Cell Dev Biol 28A 47–60

Goodwin TJ, Schroeder WL, Moyer MP (1993) Rotating-wall vessel coculture of small intestine as a prelude to tissue modeling simulated microgravity applications Proc Soc Exp Biol Med Volume 202, Feb '93

Lehninger AL (1975) The tricarboxylic acid cycle and the phosphogluconate pathway In Lehninger AL (ed) "Biochemistry" New York Worth, pp 444–448

Nilsson K, Buzsaky F, Mosbach K (1986) Growth of anchorage-dependent cells on macropourous microcarriers Bio-Technology 4 989–990

Prewett TL, Goodwin TJ, Spaulding GF (1993) Three-dimensional modeling of T-24 human bladder carcinoma cell line A new simulated microgravity vessel J Tissue Culture Methods Volume 15, Jan '93

Rodwell VW (1981) Amino acids and peptides In Martin DW, Mayes PA, Rodwell VW (eds) "Harper's Review of Biochemistry" 18th Ed California Lange Medical Publications, pp 14–21

Sanford KK, Earle WR, Evans VJ, Waltz HK, Shannon JE (1951) The measurement of proliferation in tissue cultures by enumeration of cell nuclei JNCI 11 773–795

Schwarz RP, Wolf DA (1991a) Rotating bioreactor cell culture apparatus U S Patent No 4,988,623

Schwarz RP, Wolf DA, Trinh TT (1991b) Horizontally rotated cell culture system with a coaxial tubular oxygenator U S Patent No 5,026,650

Schwarz RP, Goodwin TJ, Wolf DA (1992) Cell culture for three-dimensional modeling in rotating-wall vessels An application of simulated microgravity J Tissue Culture Methods 14 51–58

Shibayama D, Mashimo T (1972) U S Patent No 3,676,074

Thalmann E (1989) Biological experiences in bubble-free aeration system Acta Biotechnol 9 511–516

Tsao YD, Goodwin TJ, Wolf DA, Spaulding GF (1992) Responses of gravity level variations on the NASA/JSC bioreactor system Physiologist 35 49–50

Tschopp A, Cogoli A, Lewis ML, et al (1984) Bioprocessing in space Human cells attach to beads in microgravity J Biotechnol 1 287–294

van Wezel AL (1973) Microcarrier/cultures of animal cells In Kruse PF, Paterson MK (eds) "Tissue Culture Methods and Applications" New York Academic Press, pp 372–377

Vaseen VA (1980) U S Patent No 4,223,094

Wolf DA, Schwarz RP (1991) Analysis of gravity-induced particle motion and fluid perfusion flow in the NASA-designed rotating zero-head-space tissue culture vessel NASA Technical Paper 3143

Wolf DA, Schwarz RP (1992) Experimental measurement of the orbital paths of particles sedimenting within a rotating viscous fluid as influenced by gravity NASA Technical Paper 3200